



Seaweed and coastal plant biomass-stimulated methane emissions driven by methylated compound content

Ning Hall^{1,2}, Leith Murray¹, Sophie Golding-Chan¹, Riley Herron³, Wei Wen Wong¹, Katherine J. Jeppe⁴, Christopher K. Barlow⁴, Chris Greening², and Perran L. M. Cook¹

5 ¹Water Studies, School of Chemistry, Monash University, Melbourne, 3800, Australia

²Biomedicine Discovery Institute, Department of Microbiology, Monash University, Melbourne, 3800, Australia

³Australian Centre for Research on Separation Science, School of Chemistry, Monash University, Melbourne, Australia

10 ⁴Monash Proteomics and Metabolomics Platform, Department of Biochemistry and Molecular Biology, Biomedicine Discovery Institute, Monash University, Melbourne, 3800, Australia

Correspondence to: Ning Hall (ninghall0@gmail.com) and Perran L. M. Cook (perran.cook@monash.edu)

Abstract. Methane emissions from coastal sediments are increasingly influenced by ecological change, including eutrophication-driven seaweed blooms and efforts to restore coastal vegetation. Yet the pathways and variability of methane production in these environments remain poorly constrained. Here, we compared methane production from 15 three seaweeds (*Ulva*, red filamentous algae, and kelp) and three coastal plants (mangrove leaves, saltmarsh plants, and seagrass) in sands from Port Phillip Bay, Australia. To identify potential predictive precursors, we quantified key methylated osmolytes (dimethyl sulfoniopropionate (DMSP), choline, trimethylamine (TMA), trimethylamine N-oxide (TMAO)), that serve as methanogenic substrates. Methane production from seaweeds was strongly correlated with osmolyte content, whereas coastal plants, particularly mangrove leaves, stimulated methane 20 production despite low osmolyte levels, likely via decomposition pathways generating methanol. These findings broaden the understanding of organic matter sources fueling methanogenesis in coastal sediments and highlight an overlooked contribution of both seaweeds and plants to coastal methane cycling.

1 Introduction

Methane emissions from coastal waters make up the largest and most uncertain component of total marine methane 25 emissions, up to ~ 75% of total marine emissions, despite covering only ~ 15% of the total marine surface area (Weber et al., 2019; Borges et al., 2016; Rosentreter et al., 2021). A variety of processes contribute to methane supersaturation in these shallow environments, including groundwater discharge (Cable et al., 1996; Kim and Hwang, 2002), inputs from riverine and estuarine systems (Bussmann et al., 2021), and production within vegetated ecosystems such as seagrass beds, salt marshes, and mangroves (Al-Haj and Fulweiler, 2020).

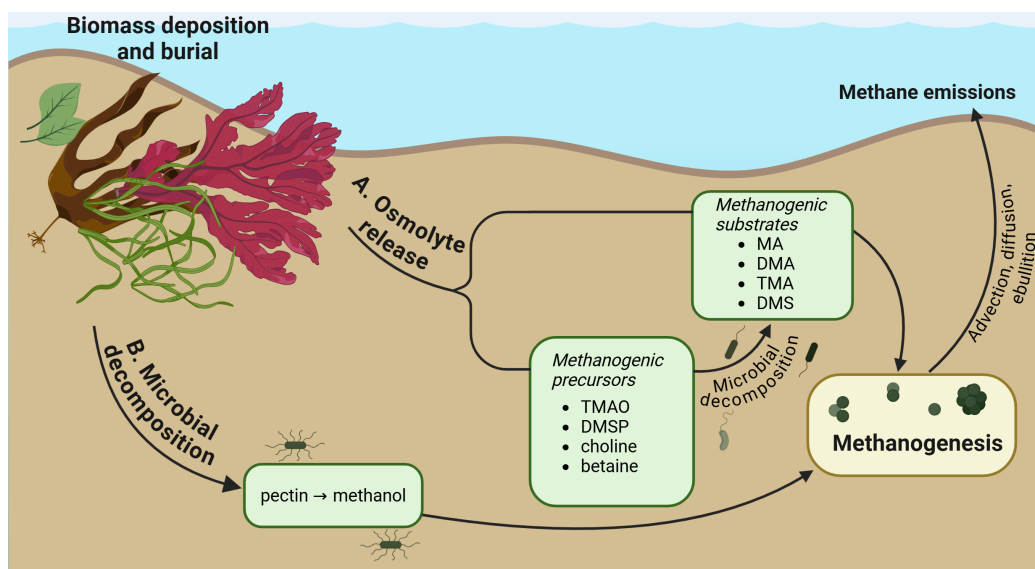
30 Recent work has shown that methylotrophic methanogenesis, methane production from methylated compounds, is a major pathway in sandy sediments, seagrass beds, and other shallow coastal sediments, especially those receiving seaweed and coastal plant inputs (Xiao et al., 2018; Tsola et al., 2021; Schorn et al., 2022; Roth et al., 2023; Hall et al., 2025). The dominance of methylotrophic methanogenesis is due to high sulfate concentrations in coastal waters competitively inhibiting acetoclastic and hydrogenotrophic methanogenesis through competition by sulfate reducing 35 bacteria for substrates acetate and hydrogen, but not methylated compounds. However, the specific methanogenic



potential of different seaweed and coastal plant species and their methylated compound composition have not been investigated.

This represents a critical knowledge gap as ecological change reshapes coastal vegetation: seaweed aquaculture is increasing at ~6% per year (Duarte et al., 2022), and is now a known potential source of methane (Deng et al., 2026), eutrophication and ocean warming is driving increasingly frequent and large macro- and microalgae blooms including *Ulva* species (Green-Gavrielidis and Thornber, 2022; Qi et al., 2025), and coastal restoration projects are re-establishing mangroves, salt marshes, and seagrasses (Buelow et al., 2022; Wang et al., 2022). On the other hand, warming oceans generally negatively affect the extent of kelp forests (Smale, 2020). Together, these changes could substantially alter methane cycling in shallow coastal zones, however without more in-depth understanding of the methane emissions stimulated by different biomass types, the direction and extent of change to marine methane emissions cannot be predicted.

Methylophilic methanogens can utilise a variety of compounds including methylamines, methylsulfides, and methanol. Methylamines, methylsulfides, and their precursors such as betaine and choline, are created in large quantities in seaweeds and coastal plants as osmolytes, playing an essential role in tolerating the osmotic stress of the marine environment (Burg and Ferraris, 2008; Yoch, 2002). These osmolytes are released on cell breakdown and are then available to methanogens in the sediment. While some of the methane produced here is oxidised before reaching the water column, the shallow and turbulent nature of shallow coastal areas mean that a substantial proportion of methane is transported to the water column through advection, ebullition, and diffusion (Santos et al., 2012; Mao et al., 2022). In addition to methylated osmolytes, decomposition processes can generate methanogenic substrates, for example, methanol is released through the hydrolysis of plant pectins (Fall and Benson, 1996; Wang et al., 2021) (Fig. 1).



60

Figure 1. Conceptual model showing pathways of methylotrophic substrate production from plant and seaweed biomass in shallow marine sediments; A. Osmolyte release occurs when stored nitrogen and sulfur based osmolytes are released on cell breakdown. These osmolytes are either used directly by methanogens (MA = methylamine, DMA = dimethylamine, TMA = trimethylamine, DMS = dimethylsulfide), or further decomposed to methanogenic substrates (TMAO = trimethylamine N-oxide, DMSP = dimethyl sulfoniopropionate); B. Decomposition breaks down pectins into methanol, which is then consumed by methylotrophic methanogens.

65

We therefore expect that methane emissions are linked to the concentration of methylated osmolytes present in the biomass upon deposition or burial, and may also be influenced by degradation processes of non-osmolyte compounds producing other methylated metabolites.

70

Specifically, we ask: (i) do seaweed and coastal plant inputs stimulate methane production to different extents, and (ii) is methane production correlated with the content of methylated osmolytes or other decomposition products, and therefore a potential proxy indicator for methane emissions of different biomass sources? Addressing these questions will improve understanding of how shifts in coastal vegetation composition and biomass influence methane emissions in marine ecosystems being rapidly changed by climate change, eutrophication, and ecological

75

restoration efforts (Trégarot et al., 2024).

2 Methods

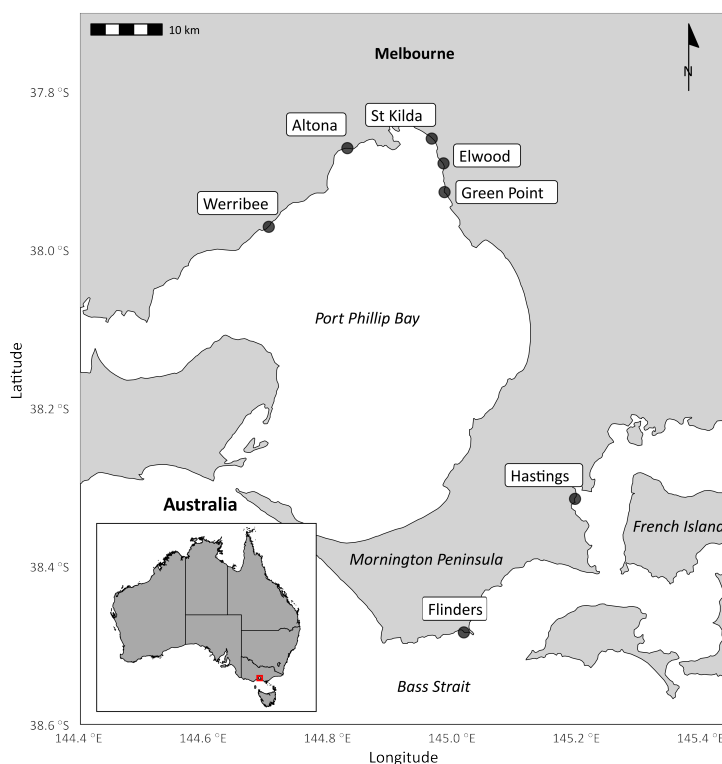
2.1 Field sites and sampling

80

Five sandy beach sites around Port Phillip Bay, Victoria, Australia were chosen for sand and seaweed collection investigating interspecies variation in methane production (Fig. 2), which was undertaken on 2nd October 2023. The sites in the western portion of the bay (Werribee and Altona) are influenced by nitrogen emissions from the Western Treatment Plant, and have historically suffered from drift algal blooms, while the eastern sites experience lower nutrient loads (Wong et al., 2022; Valero-Rodriguez et al., 2024). Three dominant types of seaweed were collected (unattached only i.e. beach-cast, not still growing) from each site to represent algal condition when it begins to



degrade. Sea lettuce (*Ulva lactuca*), and common kelp (*Ecklonia radiata*) were present at all sites. Red filamentous
85 algae (*Ceramiales*) were collected at all sites, with *Ceramicean* “*thamnions*” collected at Elwood (-37.8814,
144.9758), St Kilda (-37.8624, 144.9708) and Green Point (-37.9238, 144.9864) and *Rhodomelacean*
“*polysiphonia*” collected at Altona (-37.8714, 144.8376) and Werribee (-37.9722, 144.7004). A second field trip
was undertaken on 1st August 2024 to investigate the effect of seagrass, mangrove and salt marsh plants
(collectively “coastal plants”) on methane production. Samples of mangrove leaves (*Avicennia marina*, commonly
90 white mangrove or grey mangrove) and saltmarsh plant (*Salicornia quinqueflora*, commonly beaded samphire) were
collected from Hastings (-38.3138, 145.1958), and seagrass (*Amphibolis antarctica*, commonly wire weed or sea
nymph) was collected from Flinders (-38.4808, 145.0270). All biomass samples were transported to the lab in a cold
box and refrigerated until use. Sand was collected with acrylic cores from the intertidal zone (Werribee 2nd October
2023 trip, Flinders, 1st August 2024 trip) and transported back to the lab where the surface 0–5 cm was sectioned,
95 homogenised and sieved through a 1 mm mesh to remove shells and other large debris. This was done in order to
provide a homogenised seed population of methylotrophic methanogens which rapidly grow and drive methane
production in permeable sediments (Hall et al., 2025). Surface 0–5 cm depth was chosen as this is the sediment layer
with the highest contact with beach-cast seaweed and coastal plant biomass. Although this is some



100 **Figure 2. Map of field sites in the study. Basemap produced with data from Geoscience Australia**
(<https://pid.geoscience.gov.au/service/ga/100194>).



2.2 Slurry incubation experiments

Sand slurries were prepared in triplicate with 30 g of sand and 70 mL of unfiltered seawater weighed into a 160 mL serum vial. For samples with seaweed addition, approx. 100 mg wet weight of roughly cut up seaweed was added and the remainder frozen for metabolomic analysis. Slurries were crimp-capped with butyl rubber stoppers and the headspace purged with argon, shaken to equilibrium, and purged again to create anoxic conditions. Incubations occurred under ambient laboratory conditions (approx. 20°C, artificial day/night light cycle). Headspace samples were taken at time 0, 50, 120, 220, 320, and 460 hours for seaweeds, and 0, 21, 72, 96, 120, 170, and 180 hours for coastal plants. For controls, sand slurries were prepared in duplicate, and either had no addition of biomass or were amended with DMS (80 µM) or TMA (100 µM final concentration).

Methanol was not present in fresh mangrove leaves but rather produced over time as a breakdown product. Therefore, separate slurry incubations for methanol analysis were prepared in triplicate in 20 mL serum vials, crimp capped with butyl rubber stoppers. 5 g sand and 10 mL of seawater was used with 500 mg wet weight mangrove leaves crushed with a mortar and pestle (except for the control which contained only sand and seawater) and purged as described above to create anoxic conditions. Samples of the water were taken for methanol analysis after six days (sampling time chosen to coincide with peak methane production in previous mangrove leaf slurries) and filtered to prevent damage to the column (0.45 µm syringe filter) before analysis.

2.3 Methane analysis

Headspace methane concentration was monitored over time to determine methane production potential of the seaweeds and coastal plants. At each time point, 2 mL of helium was injected into each slurry to prevent under pressurisation, gently shaken, and a 2 mL headspace gas sample taken and injected into a helium-purged 3 mL exetainer. Samples were analysed by Gas chromatography–pulse discharge helium ionisation detection (GC–PDHID; Valco Instruments Co. Inc.). Manual triplicate five-point calibration was performed at the start of each run using NATA-accredited calibration gases from Air Liquide and BOC HiQ, along with standards and blanks every 20–30 samples to monitor for instrumental drift.

2.4 Metabolomics

For metabolomic analysis, frozen seaweed and plant samples were placed in 1.5 mL Eppendorf microtubes (kept frozen in dry ice) and crushed with a stainless-steel pestle in liquid nitrogen. 20–50 mg of crushed seaweed was then weighed frozen and extraction solvent (2:6:1 chloroform:methanol:water with 2 µM CHAPS, CAPS, PIPES and TRIS as internal standards for complex biological samples to monitor and correct for sample-to-sample differences in matrix effects caused by biomass components, differences in injection volume, and instrument response) was added at 20 µL mg⁻¹ tissue. Samples were then vortexed briefly, sonicated in an ice bath for 10 min, centrifuged at 20,000 g for 10 min at 4°C. The supernatant was then transferred to an LC-MS vial and analysed in triplicate by liquid-chromatography mass spectrometry (LC-MS). LC-MS was performed using a Vanquish Horizon coupled to a Q-Exactive Plus Orbitrap (Thermo Fisher Scientific, Australia). The chromatography used hydrophilic interaction liquid chromatography coupled to high-resolution mass spectrometry. Chromatographic separation was achieved on



a 5 μm 150 x 4.6 mm iHILIC®-(P) Classic (Hilicon, Sweden) column using with a 1290 Inline Filter, 0.3 μm (Agilent) guard column with a gradient elution of 20 mM ammonium carbonate (A) and acetonitrile (B) (linear gradient time-% B as follows: 0 min-80%, 15 min-50%, 18 min-5%, 21 min-5%, 24 min-80%, 32 min-80%) at 140 25°C. The flow rate was maintained at 500 $\mu\text{L min}^{-1}$. Samples were kept at 6°C in the autosampler and 10 μL was injected for analysis. Mass spectrometry was performed at 70,000 resolution operating in rapid switching positive (4 kV) and negative (-3.5 kV) mode electrospray ionization (capillary temperature 300°C; sheath gas flow rate 50; auxiliary gas flow rate 20; probe temp 120°C).

A seven-point calibration curve was used for quantification of TMA, TMAO, DMSP and choline, all measured 145 concentrations fell within the calibration range (Table 1). Peak integration of target metabolites was performed in Skyline 24.1. (Pino et al., 2020; MacLean et al., 2010; Skyline for Small Molecules, n.d.).

Table 1. LOD and LOQ of analytes, calculated according to ICH Harmonised Tripartite Guideline (2005).

Compound	LOD (μM)	LOQ (μM)
Choline	0.08	0.24
DMSP	1.51	4.58
TMA	0.46	1.39
TMAO	0.05	0.15

150 2.5 Methanol analysis

Methanol analysis was conducted by GC-FID (PerkinElmer Inc.). The GC was fitted with a polar ZB-WaxPlus column (30 m \times 0.32 mm internal diameter (ID) x 1.0 μm film thickness (df); Phenomenex, Inc.). The injector was operated in split mode (20:1 ratio) and heated to 120°C. Ultrahigh purity grade hydrogen (99.999%) was used as the carrier gas, with a constant flow rate of 1.5 mL min^{-1} . The initial oven temperature was set to 120°C and held for 3.5 155 min, for a total analysis time of 3.5 min. The FID temperature was set to 250°C. Samples were introduced via 1 μL manual injections of the water phase. Manual triplicate 5-point calibration was performed.

2.6 Data reporting and statistical handling

In order to relate potential methane production to methylated compound content in the initial plant sample, total methane production in the slurries was calculated using Henry's law and the headspace methane concentration at 160 460 hours for seaweeds and 180 hours for coastal plants (final time point), and divided by the dry weight of added biomass in each slurry. Concentration of osmolytes from metabolomic analysis was also normalised to the biomass dry weight.

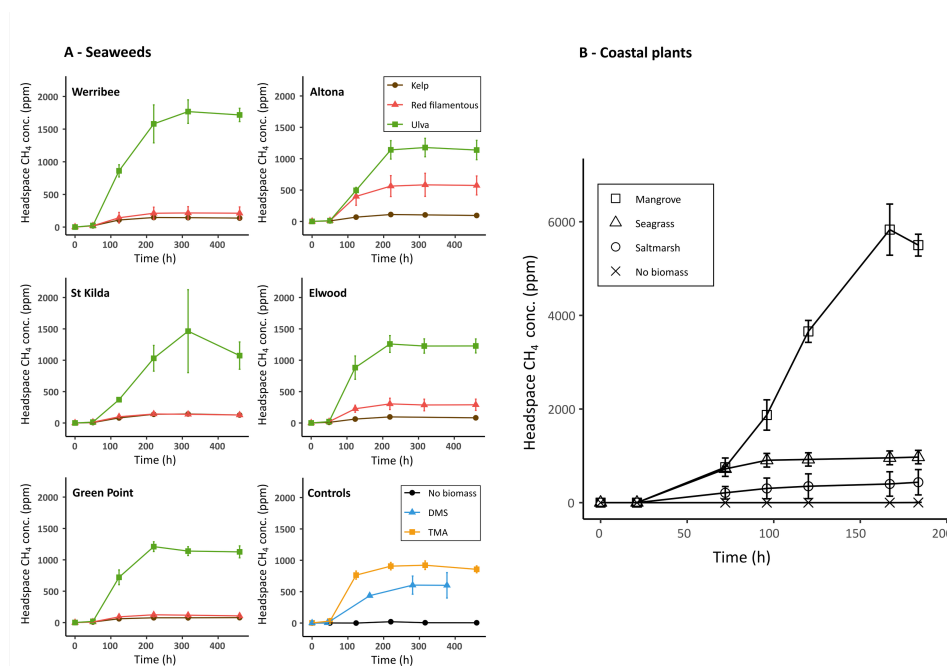
Separate simple linear regressions were conducted for TMA, TMAO, DMSP, choline, and sum of all methyl groups against the amount of methane produced in each slurry. The sum of methyl groups was calculated by multiplying the analysed concentration of each osmolyte by the number of methyl groups available to methanogens (TMA, TMAO, 165 choline = 3 methyl groups, DMSP = 2 methyl groups). All analyses were performed using the `lm()` function in R



(version 4.5.0). Model fit was assessed using adjusted R^2 values, and the statistical significance of predictor variables was evaluated at $\alpha = 0.05$.

3 Results

170 Among seaweeds, *Ulva* stimulated the most methane production in slurries, followed by red filamentous algae, and then kelp, all higher than the no biomass control (1200 ± 300 , 200 ± 200 , 100 ± 30 , and 5 ± 2 ppm at 460 hours respectively, Fig. 3A). Among coastal plants, mangrove leaves stimulated the most methane production in slurries, followed by seagrass, and then saltmarsh, also higher than the no biomass control (5500 ± 200 , 1000 ± 100 , 400 ± 300 , and 3 ± 4 ppm at 180 hours respectively, Fig. 3B). Methane concentration in the headspace had started increasing by the first sample at 50 h, increased significantly by 120 hours, and stopped increasing after 180 to 220 hours (7–10 days). DMS and TMA controls showed methane production, however only to approximately 25% of their theoretical methane production potential.

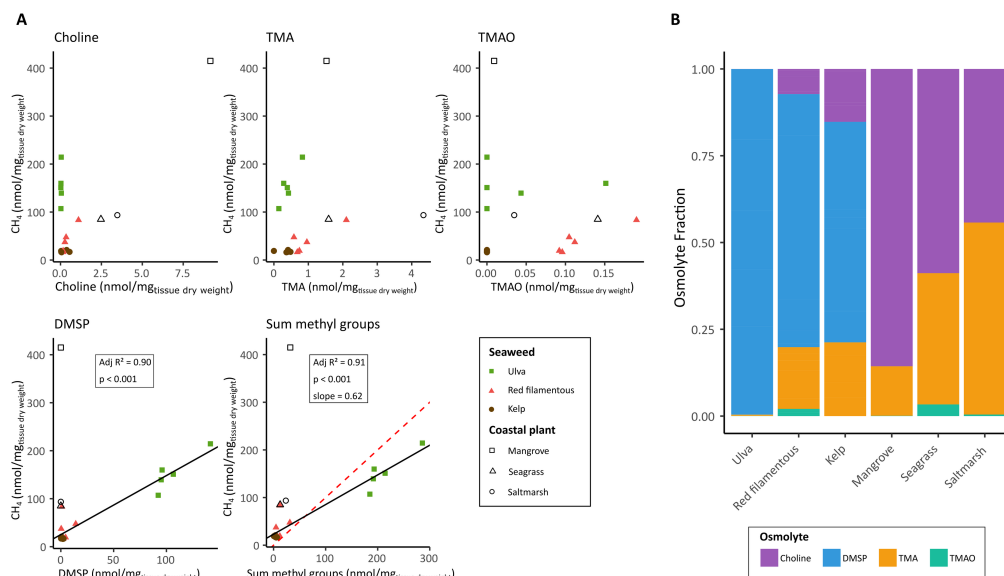


180 **Figure 3. (A – Seaweeds) Methane production from kelp, red filamentous and *Ulva* seaweed species in sand slurries from five sites around Port Phillip Bay. Seaweeds were collected locally at each site. “Controls” plot shows slurry with sand only (no added biomass), or pure DMS (dimethylsulfide) or TMA (trimethylamine) 100 μ M addition. Error bars represent standard deviations from triplicate slurries. (B – Coastal plants) Methane production from coastal plants in sand slurries. Error bars represent standard deviations from triplicate slurries.**

185 The concentration of DMSP was significantly higher in *Ulva* samples than any of the other seaweeds and higher than any other osmolyte in any seaweed. When we related osmolyte content and methane production, DMSP content correlated strongly with methane production (adj. $R^2 = 0.81$, $p < 0.001$), and was the dominant component of the



sum of methyl groups which stoichiometrically explained the total methane production, indicating that close to 100% of methyl groups were converted to methane (adj. $R^2 = 0.82$, $p < 0.001$, Fig. 4A).



190 **Figure 4. (A) Regression analysis of total methane production and osmolyte content of seaweeds, normalised by seaweed**
dry mass. Regression line only shown when significance $p < 0.05$. Coastal plants also shown on plot but not included in
regression. “Sum methyl groups” takes the sum of concentration of DMSP (dimethyl sulfoniopropionate, 2 methyl
groups), TMA (trimethylamine, 3 m. g.), TMAO (trimethylamine N-oxide, 3 m. g.), and choline (3 m. g.), multiplied by the
 195 **number of methyl groups available to methanogens. Red dashed line represents 1:1 line, representing the theoretical**
maximum methane production from analysed osmolytes. (B) Fractional osmolyte composition of each seaweed and
coastal plant species.

Despite mangrove leaves stimulating highest methane production in slurries (Fig. 3), sum methyl groups from analysed osmolytes accounted for $< 10\%$ of methane production (32 nmol/mg tissue dry weight, Fig. 4A). This sample was further analysed for methanol, which was not detected in fresh mangrove leaves; however, methanol was produced in mangrove leaf slurries with sediment and seawater, measured at 44 ± 4 nmol/mg tissue dry weight at 6 days (data not shown). The osmolyte composition differed between seaweeds and coastal plants, with DMSP composing the highest fraction in seaweeds and a combination of choline and TMA in coastal plants (Fig. 4B).

4 Discussion

4.1 Seaweed osmolyte content is strongly related to methane production potential

205 Recent work clearly shows the importance of marine plants in methane production in seaweed farms, seaweed beds, seagrass beds and seaweed wrack (Björk et al., 2023; Roth et al., 2023; Lanari et al., 2024; Dai et al., 2025; Deng et al., 2026). Emerging evidence points to methylotrophic methane production from plant osmolytes as a key driver for this (Schorn et al., 2022; Hall et al., 2025), yet no studies have provided a quantitative link between methane production potential from plant biomass and plant osmolytes. Our results clearly show that the methane production



210 potential of seaweed is closely related to osmolyte concentration, and that DMSP dominated as a methane precursor. DMSP has been previously shown to degrade to methane (Tsola et al., 2021) and this work shows that this occurs at the expected stoichiometry (1 methane molecule per methyl group) under anoxic conditions. DMS and TMA controls produced methane at less than the expected stoichiometry (approx. 25%), however this is likely due to nutrient limitation, as no biomass was added to these slurries, which provides a source of P and other micronutrients
215 to biomass amended slurries. Therefore, methylated osmolytes, and in particular DMSP, can give a relatively simple measure of methane production potential in seaweeds. The actual amount of methane produced depends on the proportion of decay of biomass that occurs under anoxic conditions. Under conditions of wrack accumulation with large potential for anoxia within the wrack, methane production has been documented to be very high, up to 176 mg m⁻² d⁻¹ (Björk et al., 2023; Lanari et al., 2024) and is likely to be close to the potential rates. Under more dispersed
220 conditions, seaweed must be exposed to anoxic conditions via burial, water column hypoxia or anoxic microsites to induce methane production, and lower but more widespread production is likely, with rates expected in the range of 0.1–5 mg m⁻² d⁻¹ under such conditions (Roth et al., 2023; Deng et al., 2026). It is also possible that leached osmolytes can be transported into anoxic zones, such as in permeable sediments (Bourke et al., 2014), leading to methane production. Further work is needed to identify likely emission factors compared to potential rates in
225 different marine environments. The fact that methane production stopped after 7–10 days, and the strong relationship with plant osmolytes, suggests that other plant components have very limited methane production potential in seaweeds. This is consistent with observations from beach wrack, which show highly variable and much lower emissions from aged wrack (Lanari et al., 2024) and suggests that methane production from seaweeds is likely to be a transient phenomenon after plant senescence. The fact that methane production was apparent but low from
230 the first time point, then increasing dramatically over the first 120 h, may be due to growth of methanogens from a small seed population being the initial rate limiting factor. Methane production from seaweeds is likely to be a transient phenomenon after plant senescence.

4.2 Changing seaweed growth patterns has consequences for coastal methane emissions

The distinct methane production potential of different seaweeds, combined with the strong relationship between
235 methane emissions and osmolyte content of seaweeds, is an important finding given these species have divergent global abundances and distributions. These patterns are especially relevant in the context of warming and increasingly eutrophic oceans, as distributions of various marine plants change rapidly (Smale and King, 2024; Qi et al., 2025). While kelp forests globally are reducing due to increasing ocean temperatures, *Ulva* blooms are becoming larger and increasingly common as they are stimulated by increasing water temperatures and high nutrient loads in
240 human-impacted areas such as the Yellow Sea (Xing et al., 2015; Cai et al., 2023; Green-Gavrielidis and Thornber, 2022). Red filamentous algae, including *polysiphonia* and *ceramium* also has the potential to bloom leading to large shoreline accumulations (Eklund et al., 2005), although the occurrence of red algal blooms is less common than *Ulva* (Joniver et al., 2021). In light of our results, this may indicate coastal biomass driven methane emissions may be predicted to rise substantially as global pressures cause the high methane potential seaweeds, *Ulva* and red
245 filamentous algae, to increase in biomass, while low-methane potential kelp declines. This predictive approach



should be expanded to other seaweed species, for example *Sargassum*, which is also increasing in growth due to changes in ocean nutrient loads in recent decades (Wang et al., 2019).

4.3 Predicting methane emissions from coastal plants

250 These results indicate that a simple analysis of methylated osmolytes in coastal plants is not sufficient to estimate potential methane emissions, as demonstrated especially by the remarkably high methane production from mangrove leaves not stoichiometrically explained by methylated osmolytes, unlike in seaweeds. Importantly, methanol was not detected in fresh leaves but only after a period of degradation, indicating that methanol was produced, possibly via breakdown of leaf pectin by bacterial or fungal pectinases (Chamier and Dixon, 1982; Ohimain, 2016). Therefore, the methanol analysed represents a dynamic pool where production and consumption processes happen
255 concurrently, and cannot be used as a quantitative predictor for methane production potential. It is possible that analysis of pectin content of plants could give a better predictor of methane potential than methylated osmolytes in coastal plants, and should be further studied.

4.4 High methane production potential from mangroves

260 Of all seaweeds and coastal plants in the study, mangroves showed the highest methane production potential by a factor of two, however these ecosystems have been shown to have significant carbon sequestration potential (Macreadie et al., 2021). Recent evidence shows mangrove ecosystems often exhibit high relative methane emissions, offsetting a large portion of their carbon sequestration capacity (Kristensen et al., 2025; Qin et al., 2025). While genomic studies indicate methylotrophic methanogenesis may be one of the primary pathways (Zhang et al., 2020), and physicochemical factors such as salinity and tide have been studied (Nazareth and Gonsalves, 2022), the
265 precise chemical precursors to methane have not previously been described. This study provides novel evidence for a mechanism by which mangrove leaves produce methane via methanol production through breakdown processes in sediments, possibly helping to explain why mangroves can be such potent hotspots of methane production.

Author contributions

NH and PLMC contributed to the conceptualization of the study. Methodology was developed by NH, WWW, PLMC, KJJ, CKB, and RH. The investigation was carried out by NH, SGC, LM, RH, and KJJ. NH was responsible for visualization. Funding was acquired by CG, PLMC, and WWW. Project administration was managed by PLMC and CKB, with PLMC and WWW also providing supervision. NH drafted the original manuscript, and all authors—
270 NH, PLMC, WWW, KJJ, CKB, RH, and LM—contributed to the review and editing of the final version.

Competing interests

275 Authors declare that they have no competing interests.



Financial support

(PLMC, CG, WWW). National Health & Medical Research Council fellowship APP1178715 (CG).

Data availability

Data are available in the Mendeley Data repository at <https://data.mendeley.com/datasets/9kj6z5h39j/1> (Dataset 1. Methane data) and <https://data.mendeley.com/datasets/73kfm8jcch/1> (Dataset 2. Metabolomics data).

References

- Al-Haj, A. N. and Fulweiler, R. W.: A Synthesis of Methane Emissions from Shallow Vegetated Coastal Ecosystems, *Global Change Biology*, 26, 2988–3005, <https://doi.org/10.1111/gcb.15046>, 2020.
- Björk, M., Rosenqvist, G., Gröndahl, F., and Bonaglia, S.: Methane Emissions from Macrophyte Beach Wrack on Baltic Seashores, *Ambio*, 52, 171–181, <https://doi.org/10.1007/s13280-022-01774-4>, 2023.
- Borges, A. V., Champenois, W., Gypens, N., Delille, B., and Harlay, J.: Massive Marine Methane Emissions from Near-Shore Shallow Coastal Areas, *Scientific Reports*, 6, 27908, <https://doi.org/10.1038/srep27908>, 2016.
- Bourke, M. F., Kessler, A. J., and Cook, P. L. M.: Influence of Buried *Ulva Lactuca* on Denitrification in Permeable Sediments, *Marine Ecology Progress Series*, 498, 85–94, <https://doi.org/10.3354/meps10611>, 2014.
- Buelow, C. A., Connolly, R. M., Turschwell, M. P., et al.: Ambitious Global Targets for Mangrove and Seagrass Recovery, *Current Biology*, 32, 1641–1649, <https://doi.org/10.1016/j.cub.2022.02.013>, 2022.
- Burg, M. B. and Ferraris, J. D.: Intracellular Organic Osmolytes: Function and Regulation, *The Journal of Biological Chemistry*, 283, 7309–7313, <https://doi.org/10.1074/jbc.R700042200>, 2008.
- Bussmann, I., Brix, H., Flöser, G., Ködel, U., and Fischer, P.: Detailed Patterns of Methane Distribution in the German Bight, *Frontiers in Marine Science*, 8, <https://doi.org/10.3389/fmars.2021.728308>, 2021.
- Cable, J. E., Bugna, G. C., Burnett, W. C., and Chanton, J. P.: Application of ^{222}Rn and CH_4 for Assessment of Groundwater Discharge to the Coastal Ocean, *Limnology and Oceanography*, 41, 1347–1353, <https://doi.org/10.4319/lo.1996.41.6.1347>, 1996.
- Cai, J., Ni, J., Chen, Z., et al.: Effects of Ocean Acidification and Eutrophication on the Growth and Photosynthetic Performances of a Green Tide Alga *Ulva Prolifera*, *Frontiers in Marine Science*, 10, <https://doi.org/10.3389/fmars.2023.1145048>, 2023.
- Chamier, A.-C. and Dixon, P. A.: Pectinases in Leaf Degradation by Aquatic Hyphomycetes: The Enzymes and Leaf Maceration, *Microbiology*, 128, 2469–2483, <https://doi.org/10.1099/00221287-128-10-2469>, 1982.
- Dai, G., Chen, X., Zhuang, G., et al.: High Methane Production and Emission From Tropical Seagrasses Through Methylophilic Methanogenesis, *Geophysical Research Letters*, 52, e2024GL113824, <https://doi.org/10.1029/2024GL113824>, 2025.
- Deng, Y., Guo, X., Hu, D., Luo, H., Chen, Y., and Zhu, X.: Methane Emission Intensifies the Warming Effect of Carbon Dioxide Efflux from a Subtropical Coastal Macroalgae Aquaculture Ecosystem, *Limnology and Oceanography*, 71, e70293, <https://doi.org/10.1002/lno.70293>, 2026.



- 310 Duarte, C. M., Bruhn, A., and Krause-Jensen, D.: A Seaweed Aquaculture Imperative to Meet Global Sustainability Targets, *Nature Sustainability*, 5, 185–193, <https://doi.org/10.1038/s41893-021-00773-9>, 2022.
- Eklund, B., Svensson, P. A., Jonsson, C., and Malm, T.: Toxic Effects of Decomposing Red Algae on Littoral Organisms, 2005.
- Fall, R. and Benson, A. A.: Leaf Methanol — the Simplest Natural Product from Plants, *Trends in Plant Science*, 1, 296–301, [https://doi.org/10.1016/S1360-1385\(96\)88175-0](https://doi.org/10.1016/S1360-1385(96)88175-0), 1996.
- 315 Green-Gavrielidis, L. A. and Thornber, C. S.: Will Climate Change Enhance Algal Blooms? The Individual and Interactive Effects of Temperature and Rain on the Macroalgae *Ulva*, *Estuaries and Coasts*, 45, 1688–1700, <https://doi.org/10.1007/s12237-022-01048-y>, 2022.
- Hall, N., Wong, W. W., Lappan, R., et al.: Coastal Methane Emissions Driven by Aerotolerant Methanogens Using Seaweed and Seagrass Metabolites, *Nature Geoscience*, 1–8, <https://doi.org/10.1038/s41561-025-01768-3>, 2025.
- 320 ICH Harmonised Tripartite Guideline: Validation of Analytical Procedures: Text and Methodology Q2(R1), 1–13, 2005.
- Joniver, C. F. H., Photiades, A., Moore, P. J., Winters, A. L., Woolmer, A., and Adams, J. M. M.: The Global Problem of Nuisance Macroalgal Blooms and Pathways to Its Use in the Circular Economy, *Algal Research*, <https://doi.org/10.1016/j.algal.2021.102407>, 2021.
- 325 Kim, G. and Hwang, D.-W.: Tidal Pumping of Groundwater into the Coastal Ocean Revealed from Submarine ²²²Rn and CH₄ Monitoring, *Geophysical Research Letters*, 29, <https://doi.org/10.1029/2002GL015093>, 2002.
- Kristensen, E., Flindt, M. R., and Quintana, C. O.: Predicting Climate Mitigation Through Carbon Burial in Blue Carbon Ecosystems—Challenges and Pitfalls, *Global Change Biology*, 31, e70022, <https://doi.org/10.1111/gcb.70022>, 2025.
- 330 Lanari, M., Busk, T., Holmer, M., et al.: From Sink to Source: Dynamic of Greenhouse Gases Emissions from Beach Wrack Accumulations in a Temperate Coastal Bay, *Science of The Total Environment*, 925, 171783, <https://doi.org/10.1016/j.scitotenv.2024.171783>, 2024.
- MacLean, B., Tomazela, D. M., Shulman, N., et al.: Skyline: An Open Source Document Editor for Creating and Analyzing Targeted Proteomics Experiments, *Bioinformatics*, 26, 966–968, <https://doi.org/10.1093/bioinformatics/btq054>, 2010.
- 335 Macreadie, P. I., Costa, M. D. P., Atwood, T. B., et al.: Blue Carbon as a Natural Climate Solution, *Nature Reviews Earth & Environment*, 2, 826–839, <https://doi.org/10.1038/s43017-021-00224-1>, 2021.
- Mao, S.-H., Zhang, H.-H., Zhuang, G.-C., et al.: Aerobic Oxidation of Methane Significantly Reduces Global Diffusive Methane Emissions from Shallow Marine Waters, *Nature Communications*, 13, 7309, <https://doi.org/10.1038/s41467-022-35082-y>, 2022.
- 340 Nazareth, D. R. and Gonsalves, M.-J.: Influence of Seasonal and Environmental Variables on the Emission of Methane from the Mangrove Sediments of Goa, *Environmental Monitoring and Assessment*, 194, 249, <https://doi.org/10.1007/s10661-021-09734-3>, 2022.
- 345 Ohimain, E. I.: Methanol Contamination in Traditionally Fermented Alcoholic Beverages: The Microbial Dimension, *SpringerPlus*, 5, 1607, <https://doi.org/10.1186/s40064-016-3303-1>, 2016.



- Pino, L. K., Searle, B. C., Bollinger, J. G., Nunn, B., MacLean, B., and MacCoss, M. J.: The Skyline Ecosystem: Informatics for Quantitative Mass Spectrometry Proteomics, *Mass Spectrometry Reviews*, 39, 229–244, <https://doi.org/10.1002/mas.21540>, 2020.
- 350 Qi, L., Wang, M., Barnes, B. B., et al.: Global Floating Algae Blooms Are Expanding, *Nature Communications*, 17, 612, <https://doi.org/10.1038/s41467-025-66822-5>, 2025.
- Qin, G., Lu, Z., Sanders, C., et al.: Mangrove Sediment Carbon Burial Offset by Methane Emissions from Mangrove Tree Stems, *Nature Geoscience*, 18, 1224–1231, <https://doi.org/10.1038/s41561-025-01848-4>, 2025.
- Rosentreter, J. A., Borges, A. V., Deemer, B. R., et al.: Half of Global Methane Emissions Come from Highly Variable Aquatic Ecosystem Sources, *Nature Geoscience*, 14, 225–230, <https://doi.org/10.1038/s41561-021-00715-2>, 2021.
- Roth, F., Broman, E., Sun, X., et al.: Methane Emissions Offset Atmospheric Carbon Dioxide Uptake in Coastal Macroalgae, Mixed Vegetation and Sediment Ecosystems, *Nature Communications*, 14, 42, <https://doi.org/10.1038/s41467-022-35673-9>, 2023.
- 360 Santos, I. R., Eyre, B. D., and Huettel, M.: The Driving Forces of Porewater and Groundwater Flow in Permeable Coastal Sediments: A Review, *Estuarine, Coastal and Shelf Science*, 98, 1–15, <https://doi.org/10.1016/j.ecss.2011.10.024>, 2012.
- Schorn, S., Ahmerkamp, S., Bullock, E., et al.: Diverse Methylophilic Methanogenic Archaea Cause High Methane Emissions from Seagrass Meadows, *Proceedings of the National Academy of Sciences*, 119, e2106628119, <https://doi.org/10.1073/pnas.2106628119>, 2022.
- 365 Skyline for Small Molecules: A Unifying Software Package for Quantitative Metabolomics, *Journal of Proteome Research*, <https://pubs.acs.org/doi/10.1021/acs.jproteome.9b00640>, n.d.
- Smale, D. A.: Impacts of Ocean Warming on Kelp Forest Ecosystems, *New Phytologist*, 225, 1447–1454, <https://doi.org/10.1111/nph.16107>, 2020.
- 370 Smale, D. A. and King, N. G.: Marine Macrophytes in a Changing World: Mechanisms Underpinning Responses and Resilience to Environmental Stress, *New Phytologist*, 244, 1675–1677, <https://doi.org/10.1111/nph.20215>, 2024.
- Trégarot, E., D’Olivo, J. P., Botelho, A. Z., et al.: Effects of Climate Change on Marine Coastal Ecosystems — A Review to Guide Research and Management, *Biological Conservation*, 289, 110394, <https://doi.org/10.1016/j.biocon.2023.110394>, 2024.
- 375 Tsola, S. L., Zhu, Y., Ghurnee, O., Economou, C. K., Trimmer, M., and Eyice, Ö.: Diversity of Dimethylsulfide-Degrading Methanogens and Sulfate-Reducing Bacteria in Anoxic Sediments along the Medway Estuary, UK, *Environmental Microbiology*, 23, 4434–4449, <https://doi.org/10.1111/1462-2920.15637>, 2021.
- Valero-Rodriguez, J. M., Dempster, T., Wong, W. W., Lewis, J. A., Cook, P. L. M., and Swearer, S. E.: Spatio-Temporal Patterns in the Biomass, Species Composition and Nitrogen Content of Drift Macroalgae in an Urbanised Coastal Embayment, *Journal of Applied Phycology*, 36, 2369–2381, <https://doi.org/10.1007/s10811-024-03249-3>, 2024.
- 380



- 385 Wang, J.-J., Li, X.-Z., Lin, S.-W., and Ma, Y.-X.: Economic Evaluation and Systematic Review of Salt Marsh Restoration Projects at a Global Scale, *Frontiers in Ecology and Evolution*, 10, <https://doi.org/10.3389/fevo.2022.865516>, 2022.
- Wang, M., Hu, C., Barnes, B. B., Mitchum, G., Lapointe, B., and Montoya, J. P.: The Great Atlantic Sargassum Belt, *Science*, 365, 83–87, <https://doi.org/10.1126/science.aaw7912>, 2019.
- Wang, Q., Alowaifeer, A., Kerner, P., et al.: Aerobic Bacterial Methane Synthesis, *Proceedings of the National Academy of Sciences*, 118, e2019229118, <https://doi.org/10.1073/pnas.2019229118>, 2021.
- 390 Weber, T., Wiseman, N. A., and Kock, A.: Global Ocean Methane Emissions Dominated by Shallow Coastal Waters, *Nature Communications*, 10, 4584, <https://doi.org/10.1038/s41467-019-12541-7>, 2019.
- Wong, W. W., Cartwright, I., Poh, S. C., and Cook, P.: Sources and Cycling of Nitrogen Revealed by Stable Isotopes in a Highly Populated Large Temperate Coastal Embayment, *Science of The Total Environment*, 806, 150408, <https://doi.org/10.1016/j.scitotenv.2021.150408>, 2022.
- 395 Xiao, K.-Q., Beulig, F., Røy, H., Jørgensen, B. B., and Risgaard-Petersen, N.: Methylotrophic Methanogenesis Fuels Cryptic Methane Cycling in Marine Surface Sediment, *Limnology and Oceanography*, 63, 1519–1527, <https://doi.org/10.1002/lno.10788>, 2018.
- Xing, Q., Tosi, L., Braga, F., Gao, X., and Gao, M.: Interpreting the Progressive Eutrophication behind the World's Largest Macroalgal Blooms with Water Quality and Ocean Color Data, *Natural Hazards*, 78, 7–21, <https://doi.org/10.1007/s11069-015-1694-x>, 2015.
- 400 Yoch, D. C.: Dimethylsulfoniopropionate: Its Sources, Role in the Marine Food Web, and Biological Degradation to Dimethylsulfide, *Applied and Environmental Microbiology*, 68, 5804–5815, <https://doi.org/10.1128/AEM.68.12.5804-5815.2002>, 2002.
- Zhang, C.-J., Pan, J., Liu, Y., Duan, C.-H., and Li, M.: Genomic and Transcriptomic Insights into Methanogenesis Potential of Novel Methanogens from Mangrove Sediments, *Microbiome*, 8, 94, <https://doi.org/10.1186/s40168-020-00876-z>, 2020.